Journal of South American Earth Sciences 26 (2008) 343–354

Contents lists available at ScienceDirect

Journal of South American Earth Sciences

journal homepage: www.elsevier.com/locate/jsames

U–Pb detrital zircon data of the Rio Fuerte Formation (NW Mexico): Its peri-Gondwanan provenance and exotic nature in relation to southwestern North America

Ricardo Vega-Granillo [a,*], Sergio Salgado-Souto [b], Saúl Herrera-Urbina [a], Víctor Valencia [c], Joaquín Ruiz [c], Diana Meza-Figueroa [a], Oscar Talavera-Mendoza [d]

[a] Departamento de Geología, Universidad de Sonora, Rosales y Encinas S/N, Hermosillo, Sonora 83000, Mexico
[b] Geociencias, Centro de Estudios Superiores del Estado de Sonora, Hermosillo, Sonora 83140, Mexico
[c] Department of Geosciences, The University of Arizona, Tucson, AZ 85721, United States
[d] Unidad Académica de Ciencias de la Tierra, Universidad Autónoma de Guerrero, A.P. 197, Taxco, Guerrero 40200, Mexico

ARTICLE INFO

Article history:
Received 9 December 2006
Accepted 30 August 2008

Keywords:
Late Ordovician
Peri-Gondwanan
Northwestern Mexico
U–Pb geochronology
Provenance

ABSTRACT

U–Pb detrital zircon studies in the Rio Fuerte Group, NW Mexico, establish its depositional tectonic setting and its exotic nature in relation to the North American craton. Two metasedimentary samples of the Rio Fuerte Formation yield major age clusters at 453–508 Ma, 547–579 Ma, 726–606 Ma, and sparse quantities of older zircons. The cumulative age plots are quite different from those arising from lower Paleozoic miogeoclinal rocks of southwestern North America and of Cordilleran Paleozoic exotic terranes such as Golconda and Robert Mountains. The relative age-probability plots are similar to some reported from the Mixteco terrane in southern Mexico and from some lower Paleozoic Gondwanan sequences, but they differ from those in the Gondwanan-affinity Oaxaca terrane. Major zircon age clusters indicate deposition in an intraoceanic basin located between a Late Ordovician magmatic arc and either a peri-Gondwanan terrane or northern Gondwanaland. The U–Pb magmatic ages of 151 ± 3 Ma from a granitic pluton and 155 ± 4 Ma from a granitic sill permit a revision of the stratigraphic and tectonic evolution of the Rio Fuerte Group. A regional metamorphism event predating the Late Jurassic magmatism is preliminarily ascribed to the Late Permian amalgamation of Laurentia and Gondwana. The Late Jurassic magmatism, deformation, and regional metamorphism are related to the Nevadan Orogeny.

1. Introduction

In the eastern El Fuerte region, northern Sinaloa, Mexico, regional metamorphosed sedimentary and volcanic sequences compose the Rio Fuerte Group (Mullan, 1978). To the west of the El Fuerte region, gneisses with minor schists and amphibolites compose the Francisco Gneiss (Mullan, 1978). The El Fuerte Group and the Francisco Gneiss are grouped either as Sonobari terrane (Campa and Coney, 1983) or as the El Fuerte block (Poole et al., 2005), although these metamorphic units are separated and their geologic relationship is unknown at this time. The Sonobari terrane mostly subcrops under thick Mesozoic and Cenozoic sequences; consequently, its nature, boundaries, age, and units, remain imprecise. The El Fuerte Group underlies the northern Guerrero terrane (Fig. 1; Campa and Coney, 1983), which is a complex of Mesozoic island arcs and interarc basins thrust over older terranes during the Late Cretaceous–Eocene Laramide Orogeny (Talavera-Mendoza and Guerrero-Suástegui, 2000). The El Fuerte region is located south of the Ouachita-Marathon-Sonora orogenic belt, which is made of Paleozoic slope and abyssal sequences (Cortés terrane; Stewart et al., 1990) thrust over mostly coeval platform sequences (Peiffer-Rangin, 1979; Poole et al., 2005) overlying an Early–Middle Proterozoic crystalline basement (Caborca terrane; Campa and Coney, 1983). According to Poole and Madrid (1988), the thrusting of slope and abyssal sequences over platform sequences occurred during Carboniferous and Late Permian times. Paleozoic metamorphic rocks of the El Fuerte region have been regarded as the internal zone of that late Paleozoic orogenic belt (Peiffer-Rangin, 1979) and as tracts of the Gondwana continent that were attached to Laurentia (Poole et al., 2005).

In this work detrital zircon crystals from the older metasedimentary units of the Rio Fuerte Group are studied through U–Pb LA-MC-ICP-MS technique in order to determine its provenance. In addition, U–Pb magmatic zircon analyses of deformed igneous rocks are made to improve the knowledge about the stratigraphy and the sequence of geological events. These data, together with available paleontological data, provide the basis for a tectonic model of this region.

* Corresponding author. Tel.: +52 662 2592110; fax: +52 662 2592111.
E-mail address: rvega@ciencias.uson.mx (R. Vega-Granillo).

0895-9811/$ - see front matter © 2008 Elsevier Ltd. All rights reserved.
doi:10.1016/j.jsames.2008.08.011

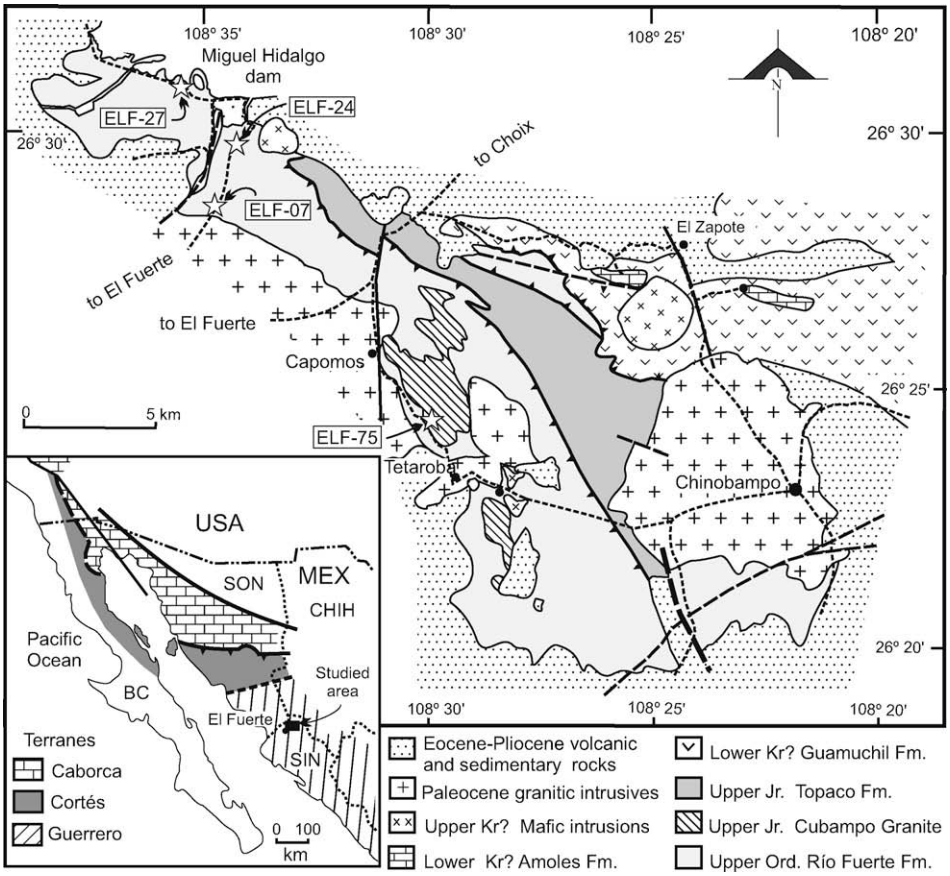

Fig. 1. Geological map of the El Fuerte region (modified from Mullan, 1978). Insert: Map of the main terranes of northwestern Mexico (adapted from Poole et al., 2005). BC: Baja California; CHIH: Chihuahua; SIN: Sinaloa; SON: Sonora.

2. Geological setting

A NW-trending belt of metasedimentary and metavolcanic rocks, surpassing 5000-m thick, crops out (Fig. 1) in northern Sinaloa, northwestern Mexico, where it is known as the Rio Fuerte Group (Mullan, 1978). This group includes the Rio Fuerte, Corral Falso, and Topaco formations (Mullan, 1978). The Rio Fuerte Formation consists of thin-bedded chert, quartzite, argillite, and a few carbonate rocks. A thin turbiditic, marbleized limestone bed in this formation yielded Mid–Late Ordovician conodonts (Poole et al., 2005). The undated Corral Falso Formation is made of finely laminated graphitic slates, phyllites and quartzites mostly indistinguishable from the Rio Fuerte Formation (Poole et al., 2005). The undated Topaco Formation consists of metasedimentary rocks at the base, which are overlain by a thick sequence of metavolcanic rocks. Mullan (1978) regards the Topaco Formation as laterally transitional with the Corral Falso Formation. Mullan (1978) separated the Rio Fuerte Formation from the overlying Corral Falso Formation based on a conspicuous rhyolite flow, less than 2 m thick, named the Nodular Rhyolite member. Mullan (1978) regards the Nodular Rhyolite also separating the upper and lower members of the Topaco Formation. The rhyolite layer borders with the metasedimentary and metavolcanic layers are straight and sharp. A summary of the previously described stratigraphy is in Fig. 2A. The meta-agglomerates forming the upper member of the Topaco Formation have clasts both of the metasedimentary rocks and the nodular rhyolite. For that reason, the contact between the Río Fuerte and the Topaco formations is considered as an angular discordance. The actual position of the Rio Fuerte Formation over the Topaco Formation and the parallelism of the foliation in both units indicate the contact is a thrust fault.

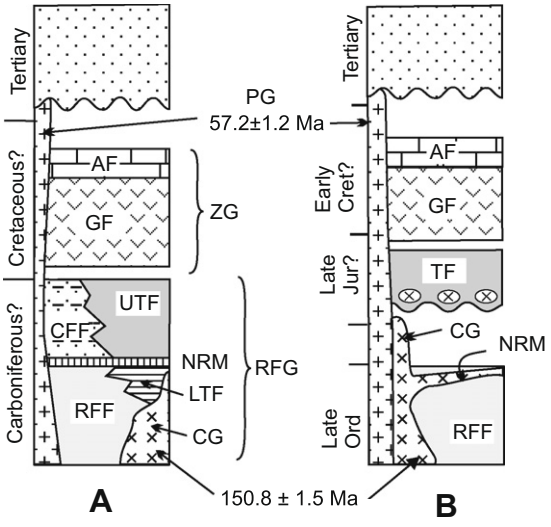

Fig. 2. Stratigraphic columns proposed by (A) Mullan (1978); (B) this article. AF: Los Amoles Formation; CFF: Corral Falso Formation; CG: Cubampo Granite; GF: Guamuchil Formation; LTF: lower member Topaco Formation; NRM: Nodular Rhyolite member; PG: Paleocene granite; RFF: Rio Fuerte Formation; RFG: Rio Fuerte Group; TF: Topaco Formation; UTF: upper member Topaco Formation; ZG: El Zapote Group.

The deformed Cubampo Granite is regarded as an intrusive equivalent of the Nodular Rhyolite member (Mullan, 1978), which intrudes into the Rio Fuerte, Corral Falso, and the lower member of the Topaco formations. Regional metamorphism mainly under greenschist facies and pervasive deformations in the Rio Fuerte Group, Cubampo Granite and Nodular Rhyolite are assigned a Late Jurassic orogenic event correlated with the Nevadan orogeny (Mullan, 1978).

The El Zapote Group includes the Guamuchil Formation consisting of volcanic rocks with a minimum thickness of 8 Km (Mullan, 1978), and the Los Amoles Formation that is made of 100 m of nonfossiliferous limestone (Mullan, 1978). This group was thrust over the Rio Fuerte Group during a Late Cretaceous-Paleocene orogenic event (Mullan, 1978). Granitic plutons with a K–Ar biotite age of 57.2 ± 1.2 Ma (Damon et al., 1983) intruded and contact metamorphosed the Rio Fuerte and El Zapote groups. Tertiary volcanic and sedimentary rocks cover all previous rocks.

3. Analytical methods

U–Pb geochronology on zircons was done by laser-ablation multicollector-inductively-coupled plasma-mass-spectrometry (LA-MC-ICPMS) at the Arizona LaserChron Center, using the procedures of Gehrels et al. (2006) for detrital zircons and Valencia et al. (2005) for magmatic zircons. For igneous samples, we mounted ~50 euhedral inclusion-free zircon crystals. The crystals are mounted in epoxy, polished to half-thickness, and imaged with cathodoluminiscence. The weighted mean of about 25-individual analyses was calculated according to Ludwing (2003). The mean age considered only the measurement of random errors (errors in $^{206}Pb/^{238}U$ and $^{206}Pb/^{204}Pb$ of each unknown). For these samples the random errors are ~0.74 Ma for ELF-75 and ~1.4 Ma for ELF-27 (2σ), and are ~0.5–1.0%. Age of standard, calibration correction from standard, composition of common Pb, and decay constant uncertainty are the other sources that contributed to the error in the final age determination. The summation of these uncertainties is the systematic error, which amount to ~1.7% in the studied samples. The error of the age for the samples is calculated adding the quadratic of both the random or measurement error and the systematic error, which is ~2.0%, ~3 Ma. All age uncertainties are reported at the 2-sigma level (2σ).

For the detrital zircon provenance analysis we mounted 500–1000 zircons in epoxy regardless of size and magnetic characteristics. The zircons are analyzed at random, with laser pits located in core portions of crystals for consistency. We analyzed 100 zircon crystals from each sample to identify the main age groups present. Data are filtered according to precision ($^{206}Pb/^{238}U$ and $^{206}Pb/^{207}$ typically 5% error cutoff) and discordance (typically 30% cutoff) and then plotted on Pb–U concordia diagrams and relative-age probability plots (using algorithms of Ludwing, 2003) or cumulative probability plots. Our interpretations derived from the data are based on the view that only clusters of age record robust source ages. This is because a single age determination may be compromised by Pb loss or inheritance (even if concordant), whereas it is unlikely that three or more grains that have experienced Pb loss or inheritance would yield the same age. For most samples, we accordingly attach age significance only to clusters defined by three or more overlapping analyses. This has particular importance for determination of the youngest age component in a detrital zircon sample, which is commonly used as a maximum depositional age. This approach also negates recent statistical treatments (e.g. Vermeesch, 2004) that report the number of analyses needed for a detrital zircon study because these treatments assume that a source can be inferred from a single analysis.

Table 1
Location of the studied samples

Sample	Coordinates UTM Zone G-12	
ELF-07	29,29,010 N	07,40,763 E
ELF-24	29,30,465 N	07,41,419 E
ELF-75	29,22,010 N	07,50,012 E
ELF-27	29,34,055 N	07,40,400 E

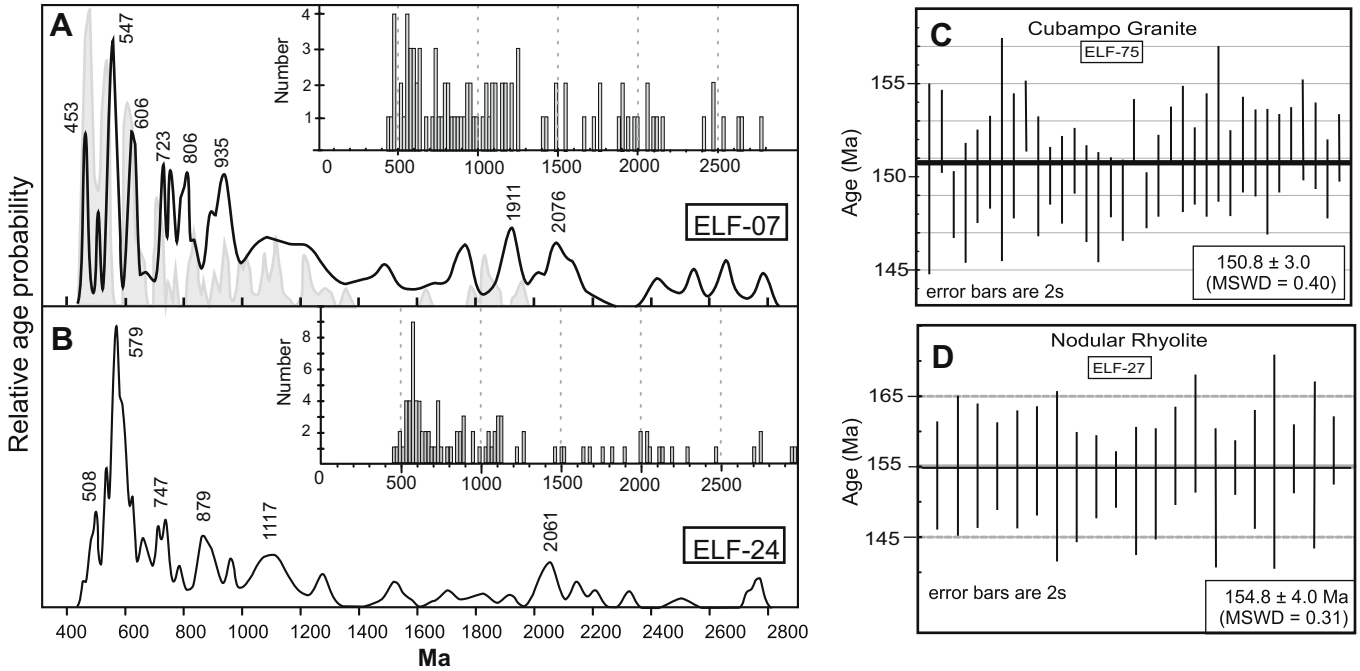

Fig. 3. Cumulative-age plots of metasedimentary rocks of the Rio Fuerte Formation. (A) Sample ELF-07, the cumulative plot for the Ixcamilpa Formation of the Mixteco terrane is plotted in grey (from Talavera-Mendoza et al., 2005); (B) sample ELF-24. Inserts in (A and B): Histograms with 20 Ma intervals. C: Weighted-average age of sample ELF-75; D: Weighted-average age of sample ELF-27.

4. Results

Two meta-sandstones were collected from the Rio Fuerte (sample ELF-07) and Corral Falso (ELF-24) formations for detrital zircon U–Pb geochronology. Sample locations are indicated in Fig. 1 and coordinates are in Table 1. In sample ELF-07, 92 zircon grains were analyzed (Fig. 3A). Ages vary from 3338 to 410 Ma. The main cluster has a 547 Ma peak, other peaks in order of importance are 453, 605, 723, 806, and 935 Ma. In the ELF-24 sample, 93 grains were analyzed and have a U/Th ratio averaging 1.57, which is typical of zircons in igneous rocks. The relative age-probability plot is in Fig. 3B. Ages vary from 2995 to 468 Ma. The major cluster has a 579 Ma peak, which included 19% of the analyzed zircons. The next peaks in order of importance are 547, 747, 879, 1117, and 2061 Ma. The complete dataset is in Table 2.

Two igneous rocks were studied by U–Pb zircon geochronology. Sample ELF-75 comes from the Cubampo Granite, which is coarse-grained granite, with conspicuous large spheroid-shaped quartz aggregates (Mullan, 1978). In this sample, 34 zircon grains were analyzed, yielding a $^{206}Pb/^{238}U$ weighted-mean-average age of 151 ± 3 Ma (2σ, MSWD = 0.40) (Fig. 3C). The ELF-27 sample comes from the Nodular Rhyolite member, where that layer divides the Rio Fuerte and Corral Falso formations. The rock is a mildly foliated metarhyolite with spheroid-quartz phenocrysts. In this rock, 25 prismatic, bipyramidal, clear pink zircons were analyzed yielding a $^{206}Pb/^{238}U$ weighted-mean-average age of 155 ± 4.0 Ma (2σ, MSWD = 0.31) (Fig. 3D). U–Th ratios of this sample vary from 1.6 to 3.3, with an average of 2.5, values which are typical of igneous rocks (Rubatto, 2002).

5. Discussion

5.1. Stratigraphic implications

Based on the younger reliable zircon cluster in sample ELF-24, the maximum depositional age for that part of the sequence is 508 Ma (Middle Cambrian), whereas in the ELF-07 sample the maximum depositional age is 453 Ma (Late Ordovician). The fossil content in the Rio Fuerte Formation indicates a Mid–Late Ordovician age for the deposit of thin limestone beds (Poole et al., 2005). Younger detrital zircon data and fossil ages constrain the time for deposition of the Rio Fuerte Formation to sometime between Middle Cambrian to Late Ordovician. The magmatic ages of the Cubampo Granite and Nodular Rhyolite have significant stratigraphic implications. The sample ELF-27 from the Nodular Rhyolite member yields a Late Jurassic age of 155±4.0 Ma. Mullan (1978) regarded this felsic rock as a rhyolite flow separating the Rio Fuerte Formation from the Corral Falso Formation, as well as the lower and upper members of the Topaco Formation (Fig. 2A). The Mid–Late Ordovician age of fossils in the Rio Fuerte Formation prevents the Nodular Rhyolite from being a volcanic flow coeval with the sedimentation; but must be a concordant sill intruded along the metasediment foliation. Consequently, the idea that rock, as a stratigraphic marker horizon, must be discarded and the separation of the Rio Fuerte Group into the Rio Fuerte and the Corral Falso formations now becomes unnecessary because they were described as practically identical and only separated by the Nodular Rhyolite member (Mullan, 1978; Poole et al., 2005). In the following paragraphs we will refer to the metasedimentary sequence as the Rio Fuerte Formation (see Table 3).

The Cubampo Granite and the Nodular Rhyolite sills have similar petrology and identical ages within errors, indicating a single magmatic event. The granite intrudes the metamorphosed Rio Fuerte Formation, and the sills are emplaced along its foliation. Thus, the granitic rocks postdate at least one regional metamorphism–deformation event and predate a later event. Dykes or sills of the Nodular Rhyolite also intrude the lower member of the Topaco Formation member, which is composed of metasedimentary rocks. For that reason, the lower member of the Topaco Formation is assigned to the Rio Fuerte Formation. The Topaco Formation term is then restricted to volcaniclastic and volcanic rocks with a predominant greenschist facies regional metamorphism, which originally made the upper member of the Topaco Formation. Fragments of the Nodular Rhyolite made part of the andesitic meta-agglomerates of this unit, implying they were extruded during the latest Jurassic, because volcanic rock and limestone of the Lower Cretaceous El Zapote Group cover it (Mullan, 1978). The significant age difference between the Mid and Upper Ordovician Rio Fuerte Formation and the Upper Jurassic Topaco Formation implies these units are unrelated, and the term Rio Fuerte Group must be dismissed. A summary of the new proposed stratigraphy is in Fig. 2B.

5.2. Zircon provenance and paleogeographic implications

The magmatic event from which the younger cluster in the ELF-07 sample (453 Ma) came was active during the Late Ordovician deposition of the Rio Fuerte sequence. Magmatic activity of that age has been reported from arcs located in the Iapetus Ocean borders. For example, the Notre Dame arc in Newfoundland existed intermittently from ca. 488 to 435 Ma (Van Staal, 2007), whereas the Popelogan-Victoria arc and the Tetagouche-Exploits back arc systems were active between 478 and 454 Ma (Van Staal, 2007). In the southern Appalachian, island arc magmatic rocks of 471–450 Ma (Coler et al., 2000) have been reported from terranes of uncertain origin or "suspect" with respect to Laurentia (Spears et al., 2004). In the Rio Fuerte samples, the main zircon clusters are 579 and 549 Ma and there is a significant peak at 606 Ma. Magmatic episodes with an age range including these peaks are common in peri-Gondwanan terranes such as the Avalonia, Carolina, or Suwannee (Nance, 1990; Wortman et al., 2000; Ingle et al., 2003). In the Avalon zone, magmatic rocks are divided into three groups; (a) about 760 Ma volcanic rocks related to ocean basins and immature island arcs, (b) 685–670 Ma arc-related felsic magmatism, (c) 635–590 Ma arc or arc-rift magmatism, and (d) 590–545 Ma contraction–extension related magmatism (O'Brien et al., 1996). In the Carolina terrane, arc to arc-rift related magmatism encompasses a period from 650 to 540 Ma (Mueller et al., 1996; Wortman et al., 2000). Zircon age clusters of 806 and 723 Ma in the Rio Fuerte rocks and the Paleoproterozoic zircons can also originate from the Pan-African–Brazilian orogen of Gondwanaland (~850–540 Ma; Da Silva et al., 2005) and its basement. In particular, peaks between 806 and 723 Ma can come from the Goias magmatic arc (e.g. Laux et al., 2005), or partially from the uncommon silicic rocks related to the Laurentian margin rifting (~760–550 Ma; Torsvick et al., 1996; Cawood et al., 2001), the latter reported in the Appalachian orogen. The source of minor clusters between 1200 and 879 Ma are Grenvillian blocks, which make part either of Laurentia or of South American Gondwana (e.g. Restrepo-Pace et al., 1997; Tohver et al., 2006).

The relative age-probability plots of the Rio Fuerte Formation differ largely from those defined in Neoproterozoic and Cambrian sequences from the southwestern United States and northwestern Mexico (Gehrels et al., 1995; Stewart et al., 2001). Plots in these sequences have larger clusters either at 1770, 1400, or 1100 Ma, matching magmatic and metamorphic events found in the southwestern Cordillera basement (Matzatzal-Yavapai, Elsonian, Grenvillian orogenies) (Irving and McGlynn, 1976; Anderson, 1989), and they are devoid of Neoproterozoic zircons. The Rio Fuerte plots also differ of those reported from those from the allochtonous Paleozoic terranes of Nevada, such as the Golconda and Robert

Table 2
U–Pb data of sample ELF-07

Sample	Corrected concentrations and ratios								Calculated ages and 1-s sd random errors					
	U (ppm)	U/Th	6/4c	7/5 ratio	±(%)	6/8 ratio	±(%)	Err.corr	6/8 Age	±(Ma)	7/5 Age	±(Ma)	6/7 Age	±(Ma)
EF07-1	170	0.9	47,604	12.19064	1.51	0.45521	1.13	0.75	2418.4	22.8	2619.2	14.2	2778	16
EF07-2	37	0.9	3243	1.52726	12.98	0.15400	1.46	0.11	923.4	12.5	941.4	79.8	984	264
EF07-3	92	0.2	7618	0.75848	14.05	0.08608	1.14	0.08	532.3	5.8	573.1	61.6	738	298
EF07-4	80	0.6	10,080	3.17943	4.04	0.24127	1.26	0.31	1393.3	15.8	1452.2	31.2	1539	72
EF07-5	70	0.6	3556	0.70809	14.39	0.08235	2.07	0.14	510.1	10.1	543.6	60.6	687	305
EF07-6	176	0.9	29,116	2.43263	2.68	0.19652	1.57	0.59	1156.6	16.6	1252.3	19.3	1421	41
EF07-7	138	0.8	3089	1.34803	7.22	0.14582	1.22	0.17	877.5	10.0	866.7	42.1	839	148
EF07-8	165	0.7	18,695	1.98174	4.46	0.18536	3.44	0.77	1096.2	34.7	1109.3	30.1	1135	56
EF07-9	170	0.8	4755	0.71908	9.59	0.08887	1.13	0.12	548.9	5.9	550.1	40.8	555	208
EF07-10	42	0.7	6531	9.87092	3.59	0.44162	2.15	0.60	2357.9	42.5	2422.8	33.1	2478	48
EF07-11	227	0.6	18,120	1.67473	3.94	0.16657	3.12	0.79	993.2	28.7	999.0	25.0	1012	49
EF07-12	314	2.4	19,684	0.76139	2.11	0.08908	1.46	0.69	550.1	7.7	574.8	9.3	674	33
EF07-13	176	0.7	18,067	2.45736	2.12	0.19235	1.00	0.47	1134.1	10.4	1259.6	15.3	1481	35
EF07-14	301	0.9	35,298	4.34577	2.08	0.29406	1.72	0.83	1661.8	25.2	1702.1	17.2	1752	22
EF07-15	56	1.9	3150	1.62664	22.38	0.15712	2.09	0.09	940.8	18.3	980.6	141.7	1071	453
EF07-16	94	0.6	5584	0.83469	14.08	0.09782	1.30	0.09	601.6	7.4	616.2	65.1	670	301
EF07-17	57	0.8	3708	1.87937	7.59	0.17561	3.88	0.51	1042.9	37.4	1073.8	50.3	1137	130
EF07-18	113	0.6	16,667	5.33997	3.53	0.32724	2.80	0.79	1825.0	44.5	1875.3	30.2	1931	39
EF07-19	49	0.6	4208	7.30567	2.81	0.39168	1.03	0.37	2130.6	18.8	2149.5	25.1	2168	46
EF07-20	120	0.9	4959	0.89003	5.91	0.09755	1.02	0.17	600.0	5.9	646.4	28.3	812	122
EF07-21	172	1.5	56,906	9.35181	2.75	0.43518	2.34	0.85	2329.0	45.7	2373.1	25.2	2411	24
EF07-22	206	4.3	9260	1.73664	3.12	0.16797	1.40	0.45	1000.9	13.0	1022.2	20.1	1068	56
EF07-23	142	0.7	7310	0.80979	5.88	0.09267	2.97	0.51	571.3	16.2	602.3	26.7	721	108
EF07-24	218	1.5	2931	0.54244	10.19	0.07266	1.28	0.13	452.2	5.6	440.0	36.4	377	228
EF07-25	51	0.5	1994	0.79596	22.64	0.07994	1.94	0.09	495.7	9.2	594.5	102.2	992	464
EF07-26	78	1.7	14,648	2.08399	4.74	0.18927	1.96	0.41	1117.4	20.1	1143.5	32.5	1193	85
EF07-27	32	0.8	3840	2.06875	12.17	0.19144	1.74	0.14	1129.2	18.1	1138.5	83.5	1156	240
EF07-28	229	2.4	79897	24.51906	2.03	0.64524	1.77	0.87	3209.6	44.7	3289.3	19.8	3338	16
EF07-29	76	1.8	14,723	2.30774	4.92	0.20432	1.27	0.26	1198.5	13.9	1214.7	34.8	1244	93
EF07-30	43	1.1	1538	3.03681	11.57	0.24704	1.83	0.16	1423.2	23.3	1416.9	88.6	1407	219
EF07-31	27	0.5	10,591	2.00760	11.47	0.18515	2.19	0.19	1095.1	22.1	1118.1	77.9	1163	224
EF07-32	1019	1.0	25,662	1.59463	2.03	0.15921	1.74	0.86	952.4	15.4	968.1	12.7	1004	21
EF07-33	137	1.7	19,095	1.50736	4.35	0.15186	2.03	0.47	911.4	17.3	933.4	26.5	986	78
EF07-34	131	1.1	9674	1.81382	4.54	0.17398	1.01	0.22	1034.0	9.6	1050.5	29.7	1085	89
EF07-35	321	1.5	29,096	6.21652	1.42	0.34791	1.00	0.71	1924.6	16.6	2006.8	12.4	2092	18
EF07-36	311	1.0	11,327	0.62413	4.16	0.08061	1.10	0.26	499.8	5.3	492.4	16.2	458	89
EF07-37	388	0.9	28,459	10.62626	2.17	0.45806	1.93	0.89	2431.0	39.1	2491.0	20.2	2540	17
EF07-38	129	2.1	11,658	1.60170	3.54	0.15712	1.94	0.55	940.7	17.0	970.9	22.1	1040	60
EF07-39	1492	9.6	30,203	0.61089	1.87	0.07467	1.57	0.84	464.2	7.0	484.1	7.2	579	22
EF07-40	190	0.8	15,819	1.36016	4.07	0.14074	2.86	0.70	848.9	22.7	871.9	23.8	931	60
EF07-41	42	0.4	3522	1.26167	12.89	0.14216	1.90	0.15	856.9	15.3	828.7	73.2	754	270
EF07-42	25	1.3	2430	1.39777	27.27	0.16489	2.68	0.10	983.9	24.5	888.0	162.8	656	592
EF07-43	61	2.3	10,259	5.20620	5.09	0.32756	1.48	0.29	1826.5	23.5	1853.6	43.4	1884	88
EF07-44	92	1.2	1917	0.61814	14.71	0.07488	1.54	0.10	465.5	6.9	488.7	57.1	599	318
EF07-45	393	1.7	64,188	6.05944	1.75	0.34703	1.43	0.82	1920.4	23.7	1984.4	15.2	2052	18
EF07-46	89	1.5	9226	1.92785	4.81	0.18357	1.57	0.33	1086.5	15.7	1090.8	32.1	1099	91
EF07-47	41	1.1	6294	3.62208	8.11	0.27468	1.00	0.12	1564.5	14.0	1554.4	64.6	1541	152
EF07-48	43	0.3	1771	1.15716	12.42	0.12870	2.40	0.19	780.4	17.7	780.6	67.7	781	257
EF07-49	87	0.7	7229	1.00616	9.69	0.11866	1.00	0.10	722.9	6.9	706.9	49.4	657	207
EF07-50	117	1.6	17,519	1.47460	3.32	0.14873	1.38	0.42	893.9	11.5	920.0	20.1	983	62
EF07-51	62	0.7	3313	0.85737	5.61	0.10124	1.63	0.29	621.7	9.7	628.7	26.3	654	115
EF07-52	76	1.6	8639	1.00479	6.21	0.11586	4.82	0.78	706.7	32.3	706.2	31.6	705	83
EF07-53	319	2.3	10,965	2.25999	5.31	0.19955	2.15	0.40	1172.9	23.1	1199.9	37.4	1249	95
EF07-54	205	1.0	44,537	5.61207	1.75	0.34566	1.43	0.82	1913.9	23.7	1918.0	15.1	1922	18
EF07-55	147	1.1	12,234	5.45169	1.43	0.33955	1.00	0.70	1884.5	16.3	1893.0	12.3	1902	18
EF07-56	115	0.8	17,662	3.98093	2.47	0.28324	1.46	0.59	1607.7	20.8	1630.3	20.1	1660	37
EF07-57	329	2.0	17,644	0.56687	4.54	0.07355	1.00	0.22	457.5	4.4	456.0	16.7	448	98
EF07-58	40	0.6	4035	1.79389	3.42	0.17056	1.20	0.35	1015.2	11.2	1043.2	22.3	1102	64
EF07-59	436	2.0	29,066	1.23977	2.16	0.13191	1.02	0.47	798.8	7.7	818.8	12.1	874	39
EF07-60	66	0.8	5118	0.86256	8.81	0.09951	1.25	0.14	611.6	7.3	631.5	41.5	704	186
EF07-61	253	2.1	5372	0.56073	6.90	0.07229	1.04	0.15	449.9	4.5	452.0	25.2	463	151
EF07-62	152	0.9	21,761	4.64468	2.45	0.31143	2.23	0.91	1747.8	34.1	1757.3	20.5	1769	18
EF07-63	372	2.1	6668	1.38558	3.81	0.13720	1.48	0.39	828.8	11.5	882.8	22.5	1021	71
EF07-64	337	3.0	108,845	11.73877	4.44	0.47758	3.84	0.86	2516.7	80.0	2583.8	41.6	2637	37
EF07-65	196	0.9	30,789	1.21251	3.15	0.13304	1.00	0.32	805.2	7.6	806.3	17.5	810	63
EF07-66	399	0.9	32,653	2.84505	2.93	0.17009	2.25	0.77	1012.6	21.1	1367.5	22.0	1976	33
EF07-67	21	0.8	3418	0.91297	5.85	0.10721	3.31	0.57	656.5	20.7	658.6	28.4	666	103
EF07-68	245	2.0	41,593	3.11551	1.54	0.24349	1.00	0.65	1404.8	12.6	1436.5	11.8	1484	22
EF07-69	182	1.5	14,412	0.76063	2.63	0.09253	1.00	0.38	570.5	5.5	574.4	11.5	590	53
EF07-70	105	0.6	23,340	5.24825	3.11	0.32889	2.36	0.76	1833.0	37.7	1860.5	26.5	1891	36
EF07-71	147	2.0	11,545	1.51920	3.63	0.15571	1.83	0.50	932.9	15.9	938.2	22.2	950	64
EF07-72	339	1.6	59,719	6.27396	1.64	0.35589	1.30	0.79	1962.7	22.0	2014.8	14.4	2069	18
EF07-73	308	1.7	9980	1.08342	2.97	0.11801	1.17	0.39	719.1	8.0	745.3	15.7	825	57
EF07-74	139	0.7	33,681	5.98655	1.51	0.35188	1.00	0.66	1943.6	16.8	1973.9	13.1	2006	20

(*continued on next page*)

Table 2 (*continued*)

Sample	Corrected concentrations and ratios								Calculated ages and 1-s sd random errors					
	U (ppm)	U/Th	6/4c	7/5 ratio	±(%)	6/8 ratio	±(%)	Err.corr	6/8 Age	±(Ma)	7/5 Age	±(Ma)	6/7 Age	±(Ma)
EF07-75	813	2.7	39,058	7.36397	1.89	0.32999	1.60	0.85	1838.3	25.6	2156.6	16.9	2475	17
EF07-76	365	1.6	53,187	6.99166	2.50	0.38397	2.29	0.92	2094.8	41.0	2110.4	22.2	2126	18
EF07-77	189	2.6	13,676	0.70869	4.89	0.08690	2.22	0.45	537.2	11.4	544.0	20.6	572	95
EF07-78	175	0.8	9543	0.85667	4.36	0.09965	1.07	0.25	612.3	6.3	628.3	20.5	686	90
EF07-79	669	14.7	16,686	0.73204	1.69	0.08998	1.00	0.59	555.4	5.3	557.8	7.3	567	30
EF07-80	310	3.3	25,482	1.14155	2.34	0.12389	1.00	0.43	752.9	7.1	773.2	12.7	832	44
EF07-81	140	0.7	10,709	0.73064	5.67	0.09342	1.71	0.30	575.8	9.4	556.9	24.3	481	119
EF07-82	189	1.3	10,201	1.03434	3.69	0.11867	1.00	0.27	722.9	6.8	721.1	19.1	715	76
EF07-83	512	1.5	78,758	11.41566	1.69	0.46070	1.36	0.81	2442.6	27.7	2557.7	15.8	2650	17
EF07-84	150	0.8	13,548	2.23997	2.28	0.19937	1.00	0.44	1171.9	10.7	1193.6	16.0	1233	40
EF07-85	326	1.2	21,588	1.09692	2.00	0.12261	1.00	0.50	745.6	7.0	751.9	10.6	771	36
EF07-86	457	1.5	9354	4.08749	2.90	0.28054	2.67	0.92	1594.1	37.7	1651.8	23.7	1726	21
EF07-87	135	2.6	13,901	2.21839	3.03	0.20003	1.00	0.33	1175.5	10.8	1186.9	21.2	1208	56
EF07-88	93	1.2	10,974	1.25395	6.04	0.12869	1.00	0.17	780.4	7.4	825.2	34.1	948	122
EF07-89	238	1.0	17,609	0.70150	3.71	0.08765	1.23	0.33	541.6	6.4	539.7	15.5	531	77
EF07-90	522	3.6	30,981	0.74375	2.13	0.09051	1.08	0.51	558.6	5.8	564.6	9.2	589	40
EF07-91	111	1.1	8853	1.63790	4.89	0.15991	1.17	0.24	956.3	10.4	984.9	30.9	1049	96
EF07-92	272	3.3	29,797	1.74357	2.64	0.17044	1.28	0.48	1014.6	12.0	1024.8	17.1	1047	47

Table 3
U–Pb data of sample ELF-24

Sample	Corrected concentrations and ratios								Calculated ages and 1-s sd random errors					
	U (ppm)	U/Th	6/4c	7/5 ratio	±(%)	6/8 ratio	±(%)	Errcorr	6/8 age	±(Ma)	7/5 age	±(Ma)	6/7 age	±(Ma)
EF24-1	336	3.5	33,017	1.90092	2.28	0.17907	1.32	0.58	1061.9	12.9	1081.4	15.2	1121	37
EF24-1	292	2.3	25,196	1.37118	2.03	0.14545	1.58	0.78	875.4	12.9	876.7	11.9	880	26
EF24-2	377	0.8	4959	2.18516	3.86	0.19350	2.42	0.63	1140.3	25.3	1176.3	26.9	1243	59
EF24-4	72	1.2	6284	2.08680	4.24	0.19396	2.08	0.49	1142.8	21.8	1144.5	29.1	1148	73
EF24-5	431	2.9	34,624	4.30646	3.64	0.29816	3.45	0.95	1682.2	51.1	1694.6	30.0	1710	22
EF24-6	213	0.6	16,741	7.89744	1.42	0.41214	1.01	0.71	2224.7	19.0	2219.4	12.8	2214	17
EF24-7	280	2.8	20,238	1.09384	5.01	0.12142	3.67	0.73	738.7	25.6	750.4	26.6	785	72
EF24-8	143	3.7	10,439	1.47495	4.62	0.14951	3.31	0.72	898.2	27.8	920.2	28.0	973	66
EF24-9	371	2.1	26,526	5.95222	2.39	0.34608	2.17	0.91	1915.8	36.0	1968.9	20.8	2025	18
EF24-10	284	2.5	18,409	0.70530	3.83	0.08843	1.24	0.32	546.2	6.5	541.9	16.1	524	79
EF24-11	229	1.6	15,094	1.38888	3.16	0.14337	1.44	0.46	863.7	11.6	884.2	18.7	936	58
EF24-12	105	1.3	51,769	17.55168	1.41	0.58066	1.00	0.71	2951.4	23.7	2965.5	13.6	2975	16
EF24-13	441	10.9	36,187	1.47558	4.71	0.15120	2.33	0.49	907.7	19.7	920.4	28.5	951	84
EF24-14	717	0.9	33,016	1.61395	1.64	0.15181	1.17	0.71	911.1	9.9	975.6	10.3	1124	23
EF24-15	188	1.7	32,517	0.85787	3.25	0.10279	1.89	0.58	630.8	11.4	629.0	15.2	622	57
EF24-16	385	1.4	15,831	1.63682	1.58	0.16221	1.10	0.70	969.0	9.9	984.5	10.0	1019	23
EF24-17	267	2.0	3760	0.81515	6.61	0.09828	1.09	0.16	604.3	6.3	605.3	30.2	609	141
EF24-18	163	1.9	11,900	1.45682	4.12	0.14775	2.49	0.60	888.4	20.7	912.7	24.8	972	67
EF24-19	300	1.3	11,697	0.74181	4.20	0.09150	2.53	0.60	564.4	13.7	563.5	18.2	560	73
EF24-20	332	1.5	13,370	0.61327	3.65	0.07864	1.06	0.29	488.0	5.0	485.6	14.1	474	77
EF24-21	811	2.4	27,691	0.98434	2.14	0.11170	1.88	0.88	682.6	12.2	695.8	10.8	739	22
EF24-22	82	0.7	18,930	0.96286	2.09	0.10929	1.51	0.72	668.6	9.6	684.8	10.4	738	30
EF24-23	283	1.2	55,774	7.14552	1.42	0.38767	1.00	0.71	2112.0	18.0	2129.7	12.6	2147	17
EF24-24	136	1.3	8612	4.94575	2.18	0.31984	1.62	0.74	1789.0	25.3	1810.1	18.4	1835	26
EF24-25	329	2.8	20,292	1.13728	3.71	0.12070	2.77	0.75	734.6	19.2	771.2	20.0	879	51
EF24-26	169	1.5	12,662	1.53959	4.21	0.15034	2.24	0.53	902.9	18.9	946.3	25.9	1049	72
EF24-27	397	2.0	27,154	0.83318	1.79	0.09949	1.44	0.80	611.4	8.4	615.4	8.3	630	23
EF24-28	247	2.6	24,806	1.21251	2.58	0.13081	1.34	0.52	792.5	10.0	806.3	14.4	845	46
EF24-29	488	5.2	46,150	3.50091	1.84	0.26769	1.53	0.83	1529.1	20.8	1527.4	14.5	1525	19
EF24-30	474	7.9	34,533	1.05531	2.05	0.11832	1.00	0.49	720.9	6.8	731.5	10.7	764	38
EF24-31	293	3.7	11,752	0.76156	2.29	0.09333	1.00	0.44	575.2	5.5	574.9	10.1	574	45
EF24-32	137	1.3	8966	0.70123	7.48	0.08776	1.01	0.13	542.3	5.2	539.5	31.3	528	163
EF24-33	81	0.6	1148	0.75072	20.27	0.09265	2.03	0.10	571.2	11.1	568.6	88.5	559	444
EF24-34	968	5.4	47,639	0.79279	1.47	0.09573	1.06	0.72	589.3	6.0	592.8	6.6	606	22
EF24-35	329	1.1	16,669	0.92698	3.33	0.11107	2.60	0.78	679.0	16.8	666.0	16.3	623	45
EF24-36	308	2.3	28,207	1.13026	2.79	0.12200	2.11	0.76	742.1	14.8	767.9	15.0	844	38
EF24-37	744	1.8	49,743	0.64154	2.22	0.08140	1.73	0.78	504.5	8.4	503.3	8.8	498	31
EF24-38	40	1.3	2475	0.86297	20.50	0.10097	2.37	0.12	620.1	14.0	631.7	96.7	674	440
EF24-39	128	1.2	1961	0.79496	10.49	0.09683	1.01	0.10	595.8	5.7	594.0	47.2	587	227
EF24-40	105	1.7	25,375	14.07814	1.42	0.52811	1.00	0.71	2733.5	22.3	2755.0	13.4	2771	16
EF24-41	425	1.5	20,231	2.26922	1.71	0.19737	1.37	0.80	1161.2	14.6	1202.8	12.0	1278	20
EF24-42	171	0.9	41,803	5.21175	1.63	0.32130	1.00	0.61	1796.1	15.7	1854.5	13.9	1921	23
EF24-43	124	2.8	26,248	4.10083	5.22	0.27282	4.85	0.93	1555.1	67.0	1654.5	42.6	1783	35
EF24-44	203	1.0	8701	1.77760	2.70	0.17759	1.01	0.37	1053.8	9.8	1037.3	17.6	1003	51
EF24-45	288	2.1	55,010	8.28204	1.42	0.40489	1.00	0.71	2191.5	18.6	2262.4	12.8	2327	17
EF24-46	87	1.5	56,74	12.89955	2.95	0.49069	2.56	0.87	2573.7	54.3	2672.3	27.8	2748	24
EF24-47	200	1.7	18,865	3.22109	4.26	0.24367	3.89	0.91	1405.7	49.1	1462.2	33.0	1545	33

Table 3 (*continued*)

Sample	Corrected concentrations and ratios							Calculated ages and 1-s sd random errors						
	U (ppm)	U/Th	6/4c	7/5 ratio	±(%)	6/8 ratio	±(%)	Errcorr	6/8 age	±(Ma)	7/5 age	±(Ma)	6/7 age	±(Ma)
EF24-48	39	0.9	4652	0.75738	4.41	0.09157	2.35	0.53	564.8	12.7	572.5	19.3	603	81
EF24-49	152	1.1	9003	3.17611	4.54	0.24893	3.16	0.70	1432.9	40.6	1451.4	35.1	1478	62
EF24-50	233	2.8	98,173	6.60462	1.49	0.37259	1.00	0.67	2041.6	17.5	2060.0	13.2	2078	20
EF24-51	337	1.4	32,549	3.90940	3.51	0.27944	2.09	0.60	1588.5	29.4	1615.6	28.4	1651	52
EF24-52	67	1.1	5695	0.77812	15.11	0.09429	1.46	0.10	580.8	8.1	584.4	67.2	598	327
EF24-53	117	2.5	8502	10.59398	3.06	0.46639	2.42	0.79	2467.7	49.6	2488.2	28.4	2505	32
EF24-54	412	5.7	37,059	0.77503	3.38	0.09269	2.64	0.78	571.4	14.4	582.6	15.0	627	46
EF24-55	169	1.3	11,215	0.79200	4.14	0.09556	1.69	0.41	588.3	9.5	592.3	18.6	608	82
EF24-56	591	14.8	26,662	0.88979	2.06	0.10352	1.00	0.49	635.0	6.0	646.3	9.8	686	38
EF24-57	192	1.8	14,735	1.79250	3.01	0.17513	1.94	0.64	1040.3	18.6	1042.7	19.6	1048	46
EF24-58	309	2.1	36,760	6.03130	3.24	0.34573	3.08	0.95	1914.2	51.0	1980.4	28.2	2050	18
EF24-59	796	2.7	32,973	0.76800	2.66	0.09314	2.24	0.84	574.1	12.3	578.6	11.7	597	31
EF24-60	98	2.0	4888	0.78578	6.42	0.09217	1.73	0.27	568.3	9.4	588.8	28.7	668	132
EF24-61	36	2.3	1950	0.85860	4.48	0.10196	1.99	0.44	625.9	11.9	629.4	21.0	642	86
EF24-62	185	10.9	11,412	0.74055	2.46	0.09138	1.00	0.41	563.7	5.4	562.7	10.6	559	49
EF24-63	387	1.8	20,274	1.14176	2.75	0.12291	1.00	0.36	747.3	7.1	773.3	14.9	849	53
EF24-64	990	2.6	44,477	0.85735	2.19	0.10006	1.81	0.83	614.8	10.6	628.7	10.2	679	26
EF24-65	318	2.4	51,390	17.43940	1.41	0.56977	1.00	0.71	2906.9	23.4	2959.3	13.6	2995	16
EF24-66	94	1.6	3128	1.84395	6.45	0.17973	1.13	0.18	1065.5	11.1	1061.3	42.5	1053	128
EF24-67	1008	0.9	4314	0.61570	2.73	0.07541	2.15	0.79	468.7	9.7	487.1	10.6	575	37
EF24-68	78	1.0	30,178	6.21801	2.11	0.36222	1.00	0.47	1992.7	17.1	2007.0	18.5	2022	33
EF24-69	235	0.7	9808	0.76111	3.59	0.09335	1.36	0.38	575.3	7.5	574.6	15.7	572	72
EF24-70	219	1.1	35,669	6.54239	1.42	0.37205	1.00	0.71	2039.0	17.5	2051.6	12.5	2064	18
EF24-71	227	1.2	10,428	1.80492	4.16	0.17127	2.90	0.70	1019.1	27.3	1047.2	27.2	1106	60
EF24-72	405	2.0	26,376	0.79924	2.62	0.09671	1.01	0.39	595.1	5.7	596.4	11.8	601	52
EF24-73	414	1.5	25,861	2.33262	1.71	0.20210	1.33	0.78	1186.6	14.4	1222.3	12.1	1286	21
EF24-74	232	2.0	13,484	1.32463	6.39	0.14189	4.78	0.75	855.4	38.3	856.5	37.0	860	88
EF24-75	244	1.8	21,864	1.61851	3.97	0.16052	2.69	0.68	959.7	24.0	977.4	24.9	1018	59
EF24-76	130	2.4	23,447	2.04807	2.60	0.19306	1.18	0.45	1137.9	12.3	1131.7	17.7	1120	46
EF24-77	153	1.9	2218	0.67630	13.38	0.08236	2.02	0.15	510.2	9.9	524.5	54.9	587	288
EF24-78	151	1.6	20,250	7.01881	2.04	0.37840	1.42	0.70	2068.8	25.1	2113.8	18.1	2158	25
EF24-79	379	3.1	47,657	1.71159	2.41	0.16630	1.80	0.75	991.7	16.5	1012.9	15.4	1059	32
EF24-80	371	3.4	11,564	0.78328	2.98	0.09405	1.00	0.34	579.4	5.5	587.4	13.3	618	61
EF24-81	660	2.5	29,308	0.65588	2.00	0.08167	1.45	0.73	506.1	7.1	512.1	8.0	539	30
EF24-82	129	2.8	8931	1.25561	5.08	0.13601	3.40	0.67	822.1	26.2	825.9	28.7	836	79
EF24-83	37	0.7	3916	1.93252	13.09	0.18012	3.33	0.25	1067.6	32.8	1092.4	87.8	1142	253
EF24-84	239	1.4	20,093	2.02458	2.10	0.18796	1.00	0.48	1110.3	10.2	1123.8	14.2	1150	37
EF24-85	136	1.9	16,686	1.92850	3.97	0.18303	1.23	0.31	1083.5	12.3	1091.0	26.5	1106	75
EF24-86	365	1.3	16,138	1.03005	3.55	0.11562	2.16	0.61	705.3	14.4	719.0	18.3	762	59
EF24-87	89	3.5	1592	0.71183	21.44	0.08658	1.46	0.07	535.3	7.5	545.8	90.7	590	469
EF24-88	396	0.8	31,280	1.80112	1.54	0.17338	1.00	0.65	1030.7	9.5	1045.9	10.1	1078	24
EF24-89	121	0.7	1703	0.93321	13.13	0.10723	1.58	0.12	656.6	9.9	669.3	64.4	712	278
EF24-90	491	1.4	9314	0.70977	5.92	0.08684	3.70	0.62	536.8	19.1	544.6	25.0	577	101
EF24-91	631	2.7	31,026	1.19310	3.82	0.12512	3.47	0.91	759.9	24.9	797.4	21.1	904	33
EF24-92	123	1.5	31,621	13.53731	1.41	0.50322	1.00	0.71	2627.6	21.6	2717.9	13.4	2786	16
EF24-93	180	1.1	3429	0.81185	4.33	0.09879	1.00	0.23	607.3	5.8	603.5	19.7	589	91

Mountains (Barbeau et al., 2005, and references therein), which have main clusters between 1.0 and 1.2 Ga or 2.6 and 2.9 Ga and are also devoid of 0.5–0.6 Ga and 0.9–1 Ga zircons, which are common in the Rio Fuerte Formation. In addition, the Rio Fuerte plots differ from those described in the Upper Cambrian–Lower Ordovician Tiñú Formation covering the Oaxacan Complex. That formation has detrital zircons only in the range of 1216 to 911 Ma (Gillis et al., 2005) and it is lacking Neoproterozoic and Cambro–Ordovician zircons.

Plots of the Rio Fuerte Formation are similar to plots from the Ixcamilpa Formation (Fig. 3A), a blueschist facies metamorphosed volcanosedimentary sequence (Talavera-Mendoza et al., 2005) from the Acatlán Complex, basement of the Mixteco terrane of southern Mexico. The Mixteco terrane is a composed terrane made of crustal fragments trapped between Laurentia and Gondwana during the closure of the Iapetus and Rheic oceans (Talavera-Mendoza et al., 2005, 2006; Vega-Granillo et al., 2007). In addition, the Rio Fuerte plots are similar to some histograms defined in lower Paleozoic rocks of Gondwana (e.g. Avigad et al., 2003; Veveers, 2004), excepting the Early Ordovician ages.

The main zircon clusters and the fossil-age range indicate the Rio Fuerte Formation was deposited during the Mid–Late Ordovician in a basin receiving detrital zircons mainly from an Upper Ordovician magmatic source and a peri-Gondwanan terrane, or from Gondwanaland (Figs. 4 and 5). The lack of Neoproterozoic zircons in the lower Paleozoic sedimentary rocks of Laurentia (e.g. Gehrels et al., 1995; Stewart et al., 2001; Fedo et al., 2003; Cawood et al., 2007) implies that peri-Gondwanan regions were separated from that paleo-continent at least until the Silurian (Van Staal, 2007). The scarcity of 1800–1600 Ma zircons in the Rio Fuerte rocks suggests a deposition basin outlaying from Laurentia, because rocks of these ages are common in the Laurentian basement (e.g. Hawkins et al., 1996). Furthermore, deposition occurred before the amalgamation of the peri-Gondwanan terranes and the Laurentian craton, which ended in the Late Silurian in the northern Appalachians (Pollock et al., 2007; Van Staal, 2007).

Fragments of the Greenville crust crop out in Colombia (Restrepo-Pace et al., 1997; Ruiz et al., 1999), which can be related to similar fragments in Mexico as the granulitic Oaxacan Complex (e.g. Ruiz et al., 1999; Solari et al., 2003, 2004) and isolated outcrops in the mexican states of Tamaulipas and Hidalgo (Ortega-Gutiérrez et al., 1995). Lower Paleozoic sedimentary sequences named Tiñú and Cañón de Caballeros formations overlay the granulitic complexes in Oaxaca and Tamaulipas respectively. These sequences

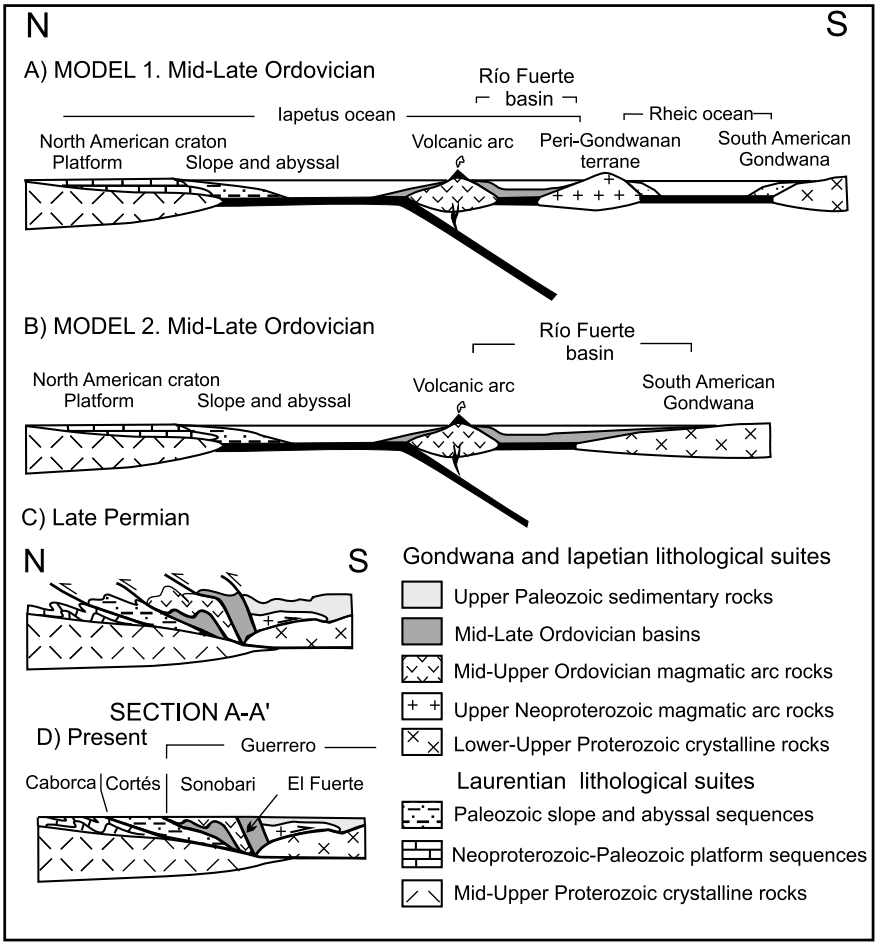

Fig. 4. (A and B) Interpretative models for the basin wherein the Rio Fuerte Formation may be deposited; (C) sketch of the Late Permian Orogeny; (D) present: Mesozoic, and Cenozoic rocks and events are not considered.

contain fossils of Gondwanan affinity (Pantoja-Alor, 1993; Stewart et al., 1999, and references therein). However, the detrital zircons of the Tiñú Formation come only from the Grenvillian rocks making its basement (Gillis et al., 2005), whereas in the Rio Fuerte Formation zircons in the range of 1285–933 Ma account for only 15% of the data. This suggests that during the Rio Fuerte deposition the basin was relatively distant, but no isolated, of Grenvillian blocks.

The predominance of Neoproterozoic and Late Ordovician zircons on the Rio Fuerte rocks indicates that an intraoceanic setting is the most suitable to explain their zircon plots. Based on both the previous statements and correlation with the tectonic settings of Neoproterozoic–lower Paleozoic magmatic rocks, two probable scenarios are proposed for the basin wherein the Rio Fuerte Formation was deposited. (1) A basin developed between a Late Ordovician island arc and a peri-Gondwanan terrane, both as main detritus sources (Fig. 4A), or (2) A basin formed between a Late Ordovician island arc and northern Gondwanaland, receiving detritus from the arc and the Pan-African–Brazilian orogen (Fig. 4B). The Late Ordovician sources can correlate with magmatic arcs bordering the eastern Iapetus Ocean as the Notre Dame or the Victoria-Popelogan arcs. Late Neoproterozoic zircons can come from peri-Gondwanan terranes formed by magmatic arcs similar to those forming the Avalon and Carolina terranes. Minor Paleo and Mesoproterozoic zircons in the Rio Fuerte sediments can arise from inherited zircons on younger magmatic rocks as indicated for the Carolina terrane (e.g. Ingle et al., 2003), or directly from a distant Gondwanaland.

5.3. Tectonic evolution

The data obtained allow us to envisage the tectonic evolution for the El Fuerte region. The Rio Fuerte Formation was deposited by the Middle–Late Ordovician in a basin located between a Late Ordovician magmatic arc and a peri-Gondwanan terrane. Continuous subduction gives rise to the closure of the ocean seaways proposed as the prolongation to Mexico of the Iapetus Oceans (Fig. 5), trapping the Rio Fuerte sequence between the North American craton and the Gondwana continent. There is not a consensus about the geographical extent of the Iapetus Ocean or even its birth place; until recently, the Early Ordovician Iapetus has been viewed as being an open ocean, bounded by Laurentia to the north, Baltica to the south and later the east, and Gondwana to the south (including peri-Gondwanan elements such as Avalonia and Armorica (Mac Niocaill et al., 1997 and references therein)). The Iapetus Ocean as defined above was closed in its north part by the Early Silurian, when peri-Gondwanan terranes collided with eastern Laurentia (Pollock et al., 2007; Van Staal, 2007). We proposed the Iapetus Ocean can extend until NW Mexico (Fig. 5) but it would be closed later than in the Appalachian chain (see Table 4).

In Sonora, thrusting of Paleozoic slope and abyssal sequences over coeval platform sequences began at the Carboniferous and ended about the Middle Permian-Early Triassic (Peiffer-Rangin, 1979; Poole and Madrid, 1988). That compressive event built a nonmetamorphosed fold-and-thrust belt (Fig. 6) known as the Ouachita-Marathon-Sonora orogenic belt (Poole et al., 2005). A first

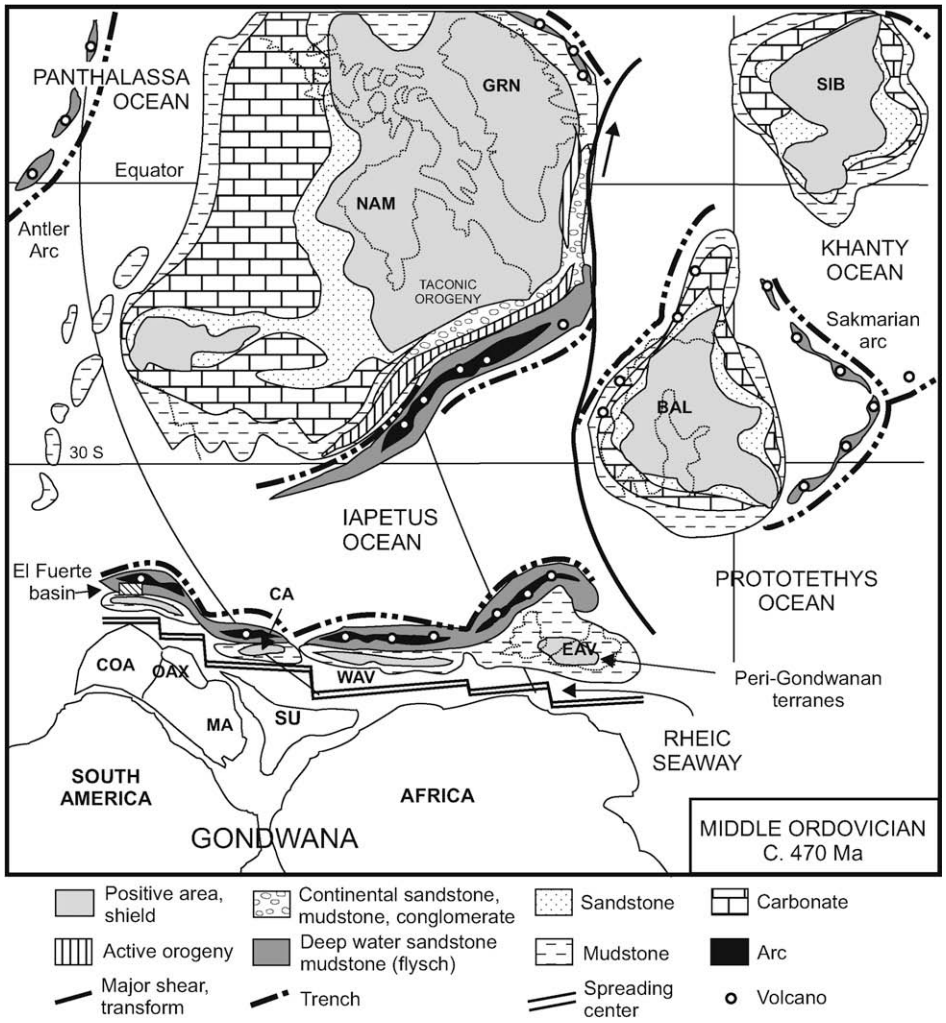

Fig. 5. Paleogeographic model for the probable location of the El Fuerte basin during the Middle Ordovician (c. 470 Ma). Continental blocks or terranes: BAL: Baltica; CA: Carolina; COA: Coahuila; EAV: Eastern Avalon; GRN: Greenland; MA: Maya; NAM: North America; OAX: Oaxaca; SIB: Siberia; SU: Suwanne; WAV: Western Avalon. Modified from Blakey (http://jan.ucc.nau.edu/~rcb7/nat.html) based in data from Cook and Bally (1975), Ross (1977), Van der Voo (1993).

metamorphic-deformational event could imprint the Rio Fuerte sequence by that time, although geochronological data to determine the age of that orogenic event are not available. Thus, a late Paleozoic orogenic event produced a fold-and-thrust belt in Sonora (external zone) and a first metamorphic-deformation event in the El Fuerte region (internal zone). This event may be likened to the Alleghanian event in the southern Appalachian resulting from the amalgamation of Gondwanan and Laurentian blocks (Fig. 4D). The internal zone in the Appalachian chain includes sequences with Laurentian or Gondwanan affinities and sequences formed within the Iapetus Ocean separating those paleocontinents (e.g. Van Staal, 1994, 2007; Hibbard et al., 2007). The internal zone in northern Mexico and the southern United States is mostly concealed under thick Mesozoic and Cenozoic sequences, but metamorphic rocks recovered from drill holes in northeastern Mexico (Stewart et al., 1999, and references therein) may be part of that zone.

By the Late Jurassic, the Cubampo pluton and Nodular Rhyolite sills intruded the previously metamorphosed Rio Fuerte Formation. Fragments of these igneous rocks were included in agglomerates of the Topaco Formation formed by the Late Jurassic. By the latest Jurassic to earliest Cretaceous, the Rio Fuerte Formation thrust over the Topaco Formation and a predominant greenschist facies metamorphic event affected both units. The Late Jurassic magmatism and the metamorphic-deformational event imprinting the Topaco Formation and overprinting the Rio Fuerte Formation can be likened to the Nevadan Orogeny, as was envisaged by Mullan (1978) based only in field observation. Volcanic and sedimentary rocks of the El Zapote Group, regarded of Early Cretaceous age, are thrust over the Rio Fuertr and Topaco formations probably during a Late Cretaceous–Paleocene Orogeny.

6. Conclusions

The Rio Fuerte Formation deposition is constrained to the Middle to Late Ordovician by the detrital zircon ages and fossil content. Detrital zircon plots have major differences with those of lower Paleozoic platform sequences of southwestern North America, indicating the exotic character of the Rio Fuerte Formation compared to the Laurentian lower Paleozoic rocks. The Rio Fuerte age plots also differ from those obtained from the Golconda and Robert Mountains terranes, which are Paleozoic terranes exotic with respect to the Cordillera, indicating the Rio Fuerte Formation has a different origin. The age plots are quite different from those obtained from the early Paleozoic cover of the Oaxaca terrane, which has a fossil content of Gondwanan affinity (Pantoja-Alor, 1993; Stewart et al., 1999, and references therein). Detrital zircon data from the Rio Fuerte Formation resemble those of the Ixcamilpa

Table 4
U–Pb data of sample ELF-75

Sample	Corrected concentrations and ratios								Calculated ages and 1-s sd random errors					
	U (ppm)	U/Th	6/4c	7/5 ratio	±(%)	6/8 ratio	±(%)	Errcorr	6/8 age	±(Ma)	7/5 age	±(Ma)	6/7 age	±(Ma)
EF75-1	289	1.5	2580	0.15151	25.83	0.02353	3.47	0.13	149.9	5.1	143.2	34.5	NA	NA
EF75-2	278	1.9	3817	0.19319	19.84	0.02393	1.46	0.07	152.5	2.2	179.4	32.6	NA	NA
EF75-3	318	1.4	2561	0.16641	12.53	0.02331	1.24	0.10	148.5	1.8	156.3	18.2	NA	NA
EF75-4	228	1.6	2658	0.15144	29.36	0.02333	2.18	0.07	148.6	3.2	143.2	39.2	NA	NA
EF75-5	325	1.3	3561	0.15386	6.72	0.02355	1.70	0.25	150.1	2.5	145.3	9.1	NA	NA
EF75-6	423	1.4	4675	0.17709	12.47	0.02367	1.67	0.13	150.8	2.5	165.6	19.1	NA	NA
EF75-7	245	1.3	785	0.14496	12.93	0.02378	4.02	0.31	151.5	6.0	137.5	16.6	NA	NA
EF75-8	326	1.5	4207	0.16722	23.69	0.02372	2.25	0.09	151.1	3.4	157.0	34.5	NA	NA
EF75-9	392	1.7	1870	0.16004	10.56	0.02406	1.26	0.12	153.3	1.9	150.7	14.8	NA	NA
EF75-10	237	1.9	2080	0.14250	36.51	0.02355	2.17	0.06	150.0	3.2	135.3	46.3	NA	NA
EF75-11	372	1.8	1290	0.14787	12.80	0.02355	1.05	0.08	150.1	1.6	140.0	16.7	NA	NA
EF75-12	222	2.0	2269	0.14778	35.42	0.02352	1.60	0.05	149.9	2.4	139.9	46.3	NA	NA
EF75-13	386	1.3	2376	0.18155	8.39	0.02368	1.21	0.14	150.9	1.8	169.4	13.1	NA	NA
EF75-14	251	1.9	2574	0.19821	17.96	0.02340	1.77	0.10	149.1	2.6	183.6	30.2	NA	NA
EF75-15	938	1.1	5457	0.15180	7.11	0.02329	2.02	0.28	148.4	3.0	143.5	9.5	NA	NA
EF75-16	407	1.5	2712	0.17699	12.87	0.02346	1.10	0.09	149.5	1.6	165.5	19.7	NA	NA
EF75-17	367	1.4	3432	0.18162	8.44	0.02335	1.48	0.18	148.8	2.2	169.5	13.2	NA	NA
EF75-18	484	1.6	11,444	0.17902	12.65	0.02394	1.15	0.09	152.5	1.7	167.2	19.5	NA	NA
EF75-19	379	1.8	2377	0.18393	12.07	0.02335	1.03	0.08	148.8	1.5	171.4	19.0	NA	NA
EF75-20	388	1.7	2293	0.16083	10.79	0.02355	1.50	0.14	150.1	2.2	151.4	15.2	NA	NA
EF75-21	641	1.3	3756	0.16607	11.62	0.02390	1.00	0.09	152.3	1.5	156.0	16.8	NA	NA
EF75-23	193	2.0	2293	0.15909	28.05	0.02378	2.28	0.08	151.5	3.4	149.9	39.1	NA	NA
EF75-24	523	1.4	3199	0.17327	6.61	0.02364	1.40	0.21	150.6	2.1	162.3	9.9	NA	NA
EF75-25	206	1.8	2951	0.18420	9.61	0.02373	2.21	0.23	151.2	3.3	171.7	15.2	NA	NA
EF75-26	293	1.8	3323	0.16263	13.85	0.02400	2.78	0.20	152.9	4.2	153.0	19.7	NA	NA
EF75-27	245	2.0	2719	0.19045	26.47	0.02358	1.55	0.06	150.2	2.3	177.0	43.0	NA	NA
EF75-28	285	2.0	2556	0.19660	14.90	0.02382	1.71	0.11	151.8	2.6	182.2	24.9	NA	NA
EF75-29	360	1.2	3107	0.16263	11.96	0.02375	1.56	0.13	151.3	2.3	153.0	17.0	NA	NA
EF75-30	139	1.4	1311	0.18980	13.99	0.02359	2.26	0.16	150.3	3.4	176.5	22.7	NA	NA
EF75-31	404	1.5	3456	0.14747	11.43	0.02375	1.40	0.12	151.3	2.1	139.7	14.9	NA	NA
EF75-32	2149	1.9	14,735	0.15879	2.34	0.02390	1.00	0.43	152.3	1.5	149.6	3.3	NA	NA
EF75-33	682	1.3	4284	0.16233	6.38	0.02395	1.79	0.28	152.6	2.7	152.7	9.0	NA	NA
EF75-34	1092	0.6	4704	0.16602	6.53	0.02381	1.55	0.24	151.7	2.3	156.0	9.4	NA	NA
EF75-35	478	1.7	3289	0.18033	8.80	0.02353	1.42	0.16	149.9	2.1	168.3	13.7	NA	NA
EF75-36	314	1.9	4611	0.19883	15.67	0.02379	1.21	0.08	151.6	1.8	184.1	26.4	NA	NA

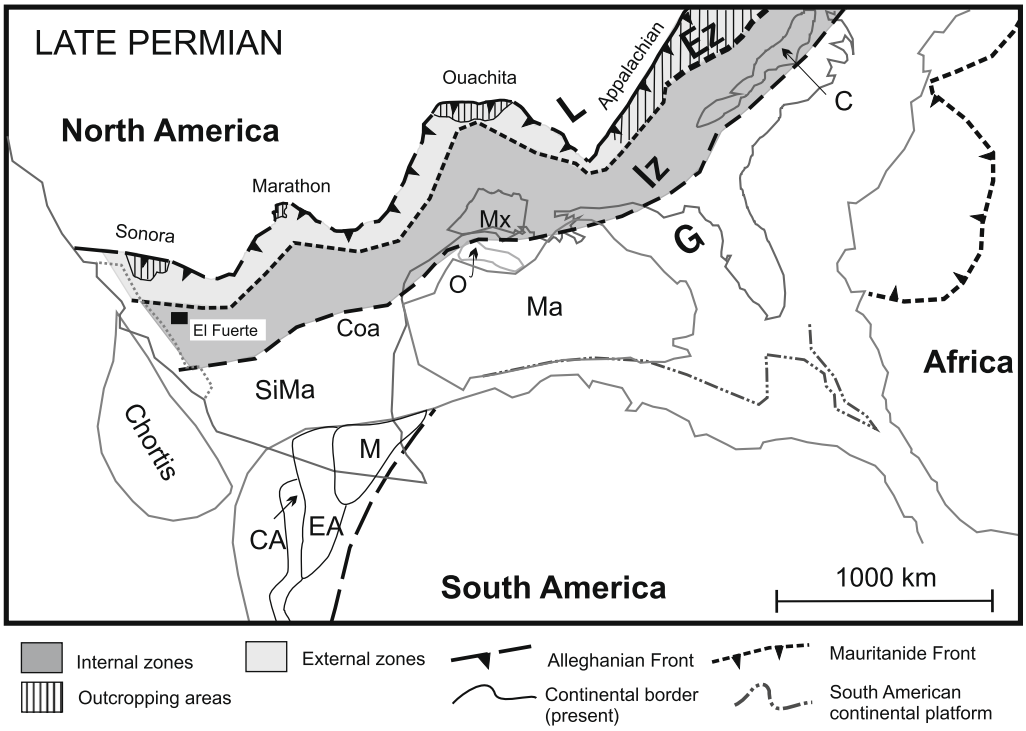

Fig. 6. Reconstruction of the Alleghanian orogen and its extension to northern Mexico. L: Laurentia; EZ: External zone of fold-and-thrusts without metamorphism; IZ: Internal zone, including metamorphic litho-tectonics suites of varied affinity; G: Gondwana. Terranes: EA: Eastern Andean; CA: Central Andean; Coa: Coahuila; O: Oaxaca; Mx: Mixteco; M: Mérida; Ma: Maya; SiMa: Sierra Madre; C: Carolina. Adapted from Pindell (1985), Poole et al. (2005); South American terranes modified from Stewart et al. (1999).

Table 5
U–Pb data of sample ELF-27

Sample	Corrected concentrations and ratios								Calculated ages and 1-s sd random errors					
	U (ppm)	U/Th	6/4c	7/5 ratio	±(%)	6/8 ratio	±(%)	Ercorr	6/8 age	±(Ma)	7/5 age	±(Ma)	6/7 age	±(Ma)
EF27-1	168	2.7	1098	0.23434	22.70	0.02414	2.53	0.11	153.8	3.8	213.8	43.8	NA	NA
EF27-2	165	2.5	1027	0.17338	36.07	0.02437	3.23	0.09	155.2	5.0	162.3	54.2	NA	NA
EF27-3	159	2.3	2712	0.17426	30.83	0.02436	2.89	0.09	155.2	4.4	163.1	46.5	NA	NA
EF27-4	296	2.2	6644	0.18498	11.77	0.02435	2.04	0.17	155.1	3.1	172.3	18.7	NA	NA
EF27-5	112	2.7	1517	0.13202	71.24	0.02429	2.73	0.04	154.7	4.2	125.9	84.6	NA	NA
EF27-7	188	2.2	2003	0.16416	24.93	0.02448	2.50	0.10	155.9	3.9	154.3	35.7	NA	NA
EF27-8	105	3.1	1295	0.18158	70.48	0.02414	3.98	0.06	153.7	6.0	169.4	110.4	NA	NA
EF27-9	202	2.7	1800	0.18468	30.99	0.02388	2.59	0.08	152.1	3.9	172.1	49.1	NA	NA
EF27-10	157	2.5	2623	0.22324	16.07	0.02412	1.94	0.12	153.6	2.9	204.6	29.8	NA	NA
EF27-12	338	2.1	4634	0.17834	15.49	0.02405	1.32	0.09	153.2	2.0	166.6	23.8	NA	NA
EF27-13	193	2.6	894	0.14911	28.58	0.02379	3.03	0.11	151.6	4.5	141.1	37.7	NA	NA
EF27-14	187	2.5	2414	0.19593	24.17	0.02396	2.61	0.11	152.6	3.9	181.7	40.2	NA	NA
EF27-16	237	2.2	2256	0.20138	23.63	0.02459	2.23	0.09	156.6	3.5	186.3	40.2	NA	NA
EF27-17	140	2.6	1852	0.19875	26.72	0.02510	2.66	0.10	159.8	4.2	184.1	45.0	NA	NA
EF27-18	184	2.5	2221	0.11162	36.26	0.02365	3.29	0.09	150.7	4.9	107.4	37.0	NA	NA
EF27-19	278	2.4	2037	0.17108	21.60	0.02433	1.25	0.06	155.0	1.9	160.4	32.1	NA	NA
EF27-20	126	3.0	1352	0.15517	45.47	0.02428	2.76	0.06	154.6	4.2	146.5	62.1	NA	NA
EF27-21	136	3.3	1195	0.19519	28.67	0.02447	4.96	0.17	155.9	7.6	181.0	47.6	NA	NA
EF27-22	306	2.2	1303	0.19108	15.29	0.02454	1.57	0.10	156.3	2.4	177.5	24.9	NA	NA
EF27-23	139	1.8	1576	0.11246	47.75	0.02437	3.88	0.08	155.2	6.0	108.2	49.1	NA	NA
EF27-25	337	1.6	2709	0.19182	28.92	0.02471	1.58	0.05	157.4	2.5	178.2	47.3	NA	NA

$^{206}Pb/^{204}Pb$ is measured ratio.
All errors are at the 1-sigma level, and include only random uncertainties.
U concentration and U/Th are calibrated by comparison with NBS SRM 610 and have uncertainty of ~25%.
Decay constants: $^{235}U = 9.8485 \times 10–10$, $^{238}U = 1.55125 \times 10–10$, $^{238}U/^{235}U = 137.88$.
Isotope ratios are corrected for Pb/U fractionation by comparison with standard zircon with an age of 564 ± 4 Ma (2-sigma).
Initial Pb composition interpreted from Stacey and Kramers (1975), with uncertainty of 1.0 for $^{206}Pb/^{204}Pb$.

suite of the Mixteco terrane in southern Mexico (Fig. 3A), which is a composed terrane constituted by crustal fragments trapped between Laurentia and Gondwana during the closure of the Iapetus and Rheic oceans (Talavera-Mendoza et al., 2005, 2006; Vega-Granillo et al., 2007). Detrital zircon plots and regional correlation suggest that the Rio Fuerte Formation was deposited in an intra-oceanic setting between an active Late Ordovician magmatic arc and either a peri-Gondwanan terrane or South American Gondwana (see Table 5).

The Cubampo Granite and Nodular rhyolite sills yielding Kimmeridgian-Tithonian ages of 155 ± 3 and 151 ± 4 Ma, intrude the previously metamorphosed Rio Fuerte Formation postdating a first regional metamorphism deformational event. This first tectono-metamorphic event on the Rio Fuerte Formation may have occured during the Carboniferous and Late Permian times when Paleozoic slope and abyssal sequences were thrust over coeval platform sequences. That orogenic event is related to the Pangea final amalgamation. The Topaco Formation volcanic rocks were extruded after 151 Ma because they include clasts of the Late Jurassic granites. A second regional metamorphism and deformational event overprints both the Rio Fuerte and Topaco formations about the latest Jurassic. The Late Jurassic magmatism, deformation, and regional metamorphism are ascribed to an orogenic event coeval to the Nevadan Orogeny.

Acknowledgements

We want to thank George Gehrels and Alexander Pullen from the LaserChron Laboratory of the University of Arizona, where the samples were dated. We also thank a former review by Fernando Barra. Thanks to Dr. Ellis Glazier for editing the English-language text.

References

Anderson, P., 1989. Stratigraphic framework, volcanic–plutonic evolution, and vertical deformation of the Proterozoic volcanic belts of central Arizona. In: Jenney, J. P., Reynolds, S.J. (Eds.), Geological Evolution of Arizona, vol. 17, Arizona Geological Society Digest , pp. 57–147.

Avigad, D., Kolodner, K., McWilliams, M., Persing, H., Weissbrod, T., 2003. Origin of northern Gondwana Cambrian sandstone revealed by detrital zircon SHRIMP dating. Geology 31 (3), 227–230.

Barbeau Jr., D.L., Ducea, M.N., Gehrels, G.E., Kidder, S., Wetmore, P.H., Saleeby, J.B., 2005. U–Pb detrital-zircon geochronology of northern Salinian basement and cover rocks. Geological Society of America Bulletin 117 (3–4), 466–481.

Campa, U.M.F., Coney, P., 1983. Tectono-stratigraphic terranes and mineral resource distributions of Mexico. Canadian Journal of Earth Sciences 20, 1040–1051.

Cawood, P.A., McCausland, P.J.A., Dunning, G.R., 2001. Opening Iapetus: constraints from the Laurentian margin in Newfoundland. Geological Society of America Bulletin 113 (4), 443–453.

Cawood, P.A., Nemchin, A.A., Strachan, R., 2007. Provenance record of Laurentian passive-margin strata in the northern Caledonides: implications for paleodrainage and paleogeography. Geological Society of American Bulletin 119, 993–1003.

Coler, D.G., Wortman, G.L., Samson, S.D., Hibbard, J.P., Stern, R., 2000. U–Pb Geochronologic, Nd Isotopic, and Geochemical Evidence for the Correlation of the Chopawamsic and Milton Terranes, Piedmont Zone, Southern Appalachian Orogen. The Journal of Geology 108 (2000), 363–380.

Cook, T.D., Bally, A.W., 1975. Stratigraphic Atlas of North and Central America. Princeton University Press, Princeton. 271 p.

Da Silva, L.C., McNaughton, N.J., Armstrong, R., Hartmann, L.A., Fletcher, I.R., 2005. The Neoproterozoic Mantiqueira Province and its African connections: a zircon-based U–Pb geochronologic subdivision for the Brasiliano/Pan-African systems of orogens. Precambrian Research 136, 203–240.

Damon, P.E., Shafiqullah, M., Roldán-Quintana, J., Cochemé, J.J., 1983. El batolito Laramide (90–40 Ma) de Sonora: Asociación de Ingenieros de Minas, Metalurgistas y Geólogos de Mexico (AIMMGM). Memoria técnica XV, Guadalajara. pp. 63–95.

Fedo, C.M., Sircombe, K.N., Rainbird, R.H., 2003. Detrital zircon analysis of the sedimentary record. Reviews in Mineralogy and Geochemistry 533, 277–303.

Gehrels, G.E., DeCelles, P.G., Ojha, T.P., Upreti, B.N., 2006. Geologic and U–Th–Pb geochronologic evidence for early Paleozoic tectonism in the Katmandu thrust sheet, central Nepal Himalaya. Geological Society of America Bulletin 118 (1–2), 185–198.

Gehrels, G.E., Dickinson, W.R., Ross, G.M., Stewart, J.H., Howell, D.G., 1995. Detrital zircon reference for Cambrian to Triassic miogeoclinal strata of western North America. Geology 23 (9), 831–834.

Gillis, R.J., Gehrels, G.E., Ruiz, J., Flores de Dios, L.A., 2005. Detrital zircon provenance of Cambrian–Ordovician and Carboniferous strata of the Oaxaca terrane, southern Mexico. Sedimentary Geology 182 (1–4), 87–100.

Hawkins, D.P., Bowring, S.A., Ilg, B.R., Karlstrom, K.E., Williams, M.L., 1996. U–Pb geochronologic constraints on Proterozoic crustal evolution. Geological Society of America Bulletin 108, 1167–1181.

Hibbard, J.P., Van Staal, C.R., Rankin, D.W., 2007. A comparative analysis of pre-Silurian crustal building blocks of the northern and the southern Appalachian orogen. American Journal of Science 307 (1), 23–45.

Ingle, S., Mueller, P.A., Heatherington, A.L., Kozuch, M., 2003. Isotopic evidence for the magmatic and tectonic histories of the Carolina terrane: implications for stratigraphy and terrane affiliation. Tectonophysics 371, 187–211.

Irving, E., McGlynn, J.C., 1976. Proterozoic magnetostratigraphy and the tectonic evolution of Laurentia. Philosophical Transactions for the Royal Society of London. Mathematical and Physical Sciences (Series A) 280 (1298), 433–467.

Laux, J.H., Pimentel, M.M., Dantas, E.L., Armstrong, R., Junges, S.L., 2005. Two Neoproterozoic crustal accretion events in the Brasilia belt, central Brazil. Journal of South American Earth Sciences 18 (2), 183–198.

Ludwing, K.R., 2003. Useŕs Manual for Isoplot 3.00. A Geochronological Toolkit for Microsoft Excel. Berkeley Geochronology Center, Berkeley, CA. Special Publication No. 4a.

Mac Niocaill, C., van der Pluijm, B.A., van der Voo, R., 1997. Ordovician paleogeography and the evolution of the Iapetus Ocean. Geology 25 (2), 159–162.

Mueller, Paul A., Kozuch, Marianne, Heatherington, Ann L., Wooden, Joseph L., Offield, Terry W., Koeppen, Robert P., Klein, Terry L., Nutman, Allen P., 1996. Evidence for Mesoproterozoic basement in the Carolina Terrane and speculations on its origin. Geological Society of America Special Paper 304, pp. 207–217.

Mullan, H.S., 1978. Evolution of the Nevadan orogen in northwestern Mexico. Geological Society of America Bulletin 89 (8), 1175–1188.

Nance, R.D., 1990. Late Precambrian–early Paleozoic arc-platform transitions in the Avalon terrane of the Northern Appalachians; review and implications. In: Sochi, A.D., Skehan, J.W., Smith, G.W. (Eds.), Geology of the Composite Avalon Terrane of Southern New England. Geological Society of America, Special Paper 245, pp. 1–12.

O'Brien, S.J., O'Brien, B.H., Dunning, G.R., Tucker, R.D., 1996. Late Neoproterozoic Avalonian and related peri-Gondwanan rocks of the Newfoundland Appalachians. In: Nance, R.D., Thompson, M.D., (Eds.), Avalonian and Peri-Gondwanan Terranes of the Circum–North Atlantic. Geological Society of America Special Paper 304, pp. 9–28.

Ortega-Gutiérrez, F., Ruiz, J., Centeno-García, E., 1995. Oaxaquia a Proterozoic microcontinent in Mexico. Geology 24, 136–198.

Pantoja-Alor, J., 1993. The Paleozoic rocks of the Nochixtlán region, State of Oaxaca. In: Ortega, G.F., Centeno G.E., Morán Z.D., Gómez, C.A. (Eds.), First Circum-Pacific and Circum-Atlantic Terrane Conferance. Terrane Geology of Southern Mexico. Guidebook of Field Trip B. pp. 84–91.

Peiffer-Rangin, F., 1979. Les zones isopiques du Paléozoique inférieur du NW Mexicain. Temoins du relais entre les Appalaches et la cordillère ouest-américaine. Comptes Rendus Academie Sciences Paris t 288, série D, pp. 1517–1519.

Pindell, J.L., 1985. Alleghenian reconstruction and subsequent evolution of the Gulf of Mexico, Bahamas, and Proto-Caribbean. Tectonics 4 (1), 1–39.

Poole, F.G., Madrid, R.J., 1988. Allochtonous Paleozoic eugeoclinal rocks of the Barita de Sonora mine area, central Sonora, Mexico. In: Rodríguez Torres, R. (Ed.), El Paleozoico de la región central del Estado de Sonora: Libreto Guía de la Excursión para el segundo simposio sobre la geología y minería en el Estado de Sonora. Instituto de Geología, UNAM, pp. 32–41.

Poole, F.G., Perry Jr., W.J., Madrid, R.J., Amaya-Martínez, R., 2005. Tectonic synthesis of the Ouachita-Marathon-Sonora orogenic margin of southern Laurentia: stratigraphic and structural implications for timing of deformational events and plate-tectonic model. Geological Society of America Special Paper 393, 543–596.

Pollock, J.C., Wilton, D.H.C., Van Staal, C.R., Morrissey, K.D., 2007. U–Pb detrital zircon geochronological constraints on the Early Silurian collision of Ganderia and Laurentia along the Dog Bay Line: the terminal Iapetan suture in the Newfoundland Appalachians. American Journal of Science 307 (2), 399–433.

Restrepo-Pace, A., Ruiz, J., Gehrels, G., Cosca, M., 1997. Geochronology and Nd isotopic data of Grenville-age rocks in the Colombian Andes: new constraints for Late Proterozoic–early Paleozoic paleocontinental reconstructions of the Americas. Earth and Planetary Science Letters 150 (3–4), 427–441.

Ross, R.J., 1977. Ordovician paleogeography of the western United States. In: Stewart, J.H., Stevens, C.H., Fritsche, A.E. (Eds.), Paleozoic Paleogeography of the Western United States, Pacific Section SEPM Symposium 1, pp. 19–38.

Rubatto, D., 2002. Zircon trace element geochemistry: distribution coefficients and the link between U–Pb ages and metamorphism. Chemical Geology 184 (1–2), 123–138.

Ruiz, J., Tosdal, R.M., Restrepo, P.A., Murillo-Muñetón, G., 1999. Pb isotope evidence for Colombian–southern México connections in the Proterozoic. In: Ramos, V.A., Keppie, J.D. (Eds.), Laurentia–Gondwana Connections before Pangea. Geological Society of America Special Paper 336, pp. 183–198.

Solari, L.A., Keppie, J.D., Ortega-Gutierrez, F., Cameron, K.L., Lopez, R., 2004. U–Pb zircon geochronology and the behaviour of common Pb isotopes in the northern Oaxacan Complex, southern Mexico: implications for the age and origin of Oaxaquia. Revista Mexicana de Ciencias Geológicas 21–2, 212–225.

Solari, L.A., Keppie, J.D., Ortega, G.F., Cameron, K.L., Lopez, R., Hames, W.E., 2003. 990 and 1100 Ma Grenvillian tectonothermal events in the northern Oaxacan Complex, southern México: roots of an orogen. Tectonophysics 365, 257–282.

Spears, D.B., Owens, B.E, Bailey, C.M., 2004. The Goochland-Chopawamsic terrane boundary, Central Virginia Piedmont. In: Geology of the National Capital Region-field Trip Guidebook, USGS Circular 1264, pp. 223–245.

Stacey, J.S., Kramers, J.D., 1975. Approximation of terrestial lead isotope evolution by two-stage model. Earth and Planetary Science Letters 26, 207–221.

Stewart, J.H., Gehrels, G., Barth, A.P., Link, P.K., Christie-Blick, N., Wrucke, C.T., 2001. Detrital zircon provenance of Mesoproterozoic to Cambrian arenites in the western United States and northwestern Mexico. Geological Society of America Bulletin 113 (10), 1343–1356.

Stewart, J.H., Blodgett, R.B., Boucout, A.J., Carter, J.L., López, R., 1999. Exotic Paleozoic strata of Gondwana provenance near Ciudad Victoria, Tamaulipas, Mexico. In: Ramos, V.A., Keppie, J.D. (Eds.), Laurentia–Gondwana Connections before Pangea. Geological Society of America Special Paper 336, pp. 227–252.

Stewart, J.H., Poole, F.G., Ketner, K.B., Madrid, R.J., Roldan-Quintana, J., Amaya-Martinez, R., 1990. Tectonics and stratigraphy of the Paleozoic and Triassic southern margin of North America, Sonora, Mexico. In: Gehrels, G., Spencer, J. (Eds.), Geological Excursions through the Sonoran Desert Region, Arizona and Sonora. Arizona Geological Survey Special Paper 7, pp. 83–195.

Talavera-Mendoza, O., Guerrero-Suástegui, M., 2000. Geochemistry and isotopic composition of the Guerrero Terrane (western Mexico): implications for the tectono-magmatic evolution of the southwestern North America during the Late Mesozoic. Journal of South American Earth Sciences 13 (4), 297–324.

Talavera-Mendoza, O., Ruiz, J., Gehrels, G.E., Meza-Figueroa, D., Vega-Granillo, R., Campa-Uranga, M.F., 2005. U–Pb geochronology of the Acatlán Complex and implications for the Paleozoic paleogeography and tectonic evolution of southern Mexico. Earth and Planetary Science Letters 235 (3–4), 682–699.

Talavera-Mendoza, O., Ruiz, J., Gehrels, G.E., Meza-Figueroa, D.M., Vega-Granillo, R., Valencia, V.A., 2006. Reply to comment on "U–Pb geochronology of the Acatlán Complex and implications for the Paleozoic paleogeography and tectonic evolution of southern Mexico" by Talavera et al.. Earth and Planetary Science Letters 245, 476–480.

Tohver, E., Teixeira, W., van der Pluijm, B., Geraldes, M.C., Bettencourt, J.S., 2006. Restored transect across the exhumed Grenville orogen of Laurentia and Amazonia, with implications for crustal architecture. Geology 34 (8), 669–672.

Torsvick, T.H., Smethurst, M.A., Meert, J.G., Van der Voo, R., McKerrow, W.S., Brasier, M.D., Sturt, B.A., Walderhaug, H.J., 1996. Continental break-up and collision in the Neoproterozoic and Paleozoic – a tale of Baltica and Laurentia. Earth-Science Reviews 40, 229–258.

Valencia, V.A., Ruiz, J., Barra, F., Geherls, G., Ducea, M., Titley, S.M., Ochoa-Landin, L., 2005. U–Pb single zircon and Re–Os geochronology from La Caridad Porphyry copper deposit: insights for the duration of magmatism and mineralization in the Nacozari District, Sonora, Mexico. Mineralium Deposita 40, 175–191.

Van der Voo, R., 1993. Paleomagnetism of the Atlantic, Tethys, and Iapetus Oceans. Cambridge University Press, Cambridge. 411 p.

Van Staal, C.R., 1994. Brunswick subduction complex in the Canadian Appalachians: record of the Late Ordovician to Late Silurian collision between Laurentia and the Gander margin of Avalon. Tectonics 13 (4), 946–962.

Van Staal, C.R., 2007. Pre-Carboniferous metallogeny of the Canadian Appalachians. In: Goodfellow, W.D. (Ed.), Mineral Resources of Canada: A Synthesis of Major Deposit-types, District Metallogeny, the Evolution of Geological Provinces, and Exploration Method. Mineral Deposit Division, Geological Association of Canada, Special Publication vol. 5, pp. 793-818.

Vega-Granillo, R., Talavera-Mendoza, O., Meza-Figueroa, D., Ruiz, J., Gehrels, G.E., López-Martínez, M., 2007. P-T-t evolution of Paleozoic high-P rocks of the Acatlán Complex (southern Mexico): implications for the evolution of the Iapetus and Rheic oceans. Geolological Society of America Bulletin 119 (9), 1249–1264.

Vermeesch, P., 2004. How many grains are needed for a provenance study? Earth and Planetary Science Letters 224 (3–4), 441–451.

Veveers, J.J., 2004. Gondwanaland from 650 to 500 Ma assembly through 320 Ma merger in Pangea to 185–100 Ma breakup: supercontinental tectonics via stratigraphy and radiometric dating. Earth-Sciences Reviews 68 (1–2), 1–132.

Wortman, G.L., Samson, S.D., Hibbard, J.P., 2000. Precise U–Pb zircon constraints on the earliest magmatic history of the Carolina terrane. Journal of Geology 108 (3), 321–338.